Research Article

Evaluation of titanium dioxide and tantalum pentoxide nanoparticles for coating NiTi archwires in orthodontics: An in vitro study

Abeer Basim Mahmood[1], **Akram Faisal Alhuwaizi**[1], **Mohammed K. Khalaf**[2], **Abbas R. Zaher**[3]

1 Department in Orthodontic, College of Dentistry, University of Baghdad, Baghdad, Iraq
2 Center of Applied Physics, Directorate of Materials Research, Ministry of Higher Education and Scientific Research /Science and Technology, Baghdad, Iraq
4 Department in Orthodontic College of Dentistry University of Alexandria, Egypt
*Correspondence: dr_abeerbasim@coadental.uobaghdad.edu.iq

Received date: 15-10-2023
Accepted date: 02-01-2024
Published date: 15-09-2024

Article DOI

Abstract: Background: This study aims to enhance the biocompatibility of Nickel–Titanium (NiTi) alloy by developing a new coating using titanium dioxide (TiO_2) and titanium pentoxide (Ta_2O_5) through direct current (DC) reactive sputtering technology. Materials and methods: Two distinct coating materials, namely, TiO_2 and Ta_2O_5, were used to fabricate NiTi orthodontic archwires with improved surface properties. TiO_2 nanoparticles, with thickness ranging from 21.90 nm to 31.93 nm, were deposited onto NiTi alloy substrates through DC reactive sputtering deposition under different power conditions. Results: X-ray diffraction and field emission scanning electron microscopy validated the uniformity and morphology of the coatings. Immersion tests in simulated body fluid (SBF) revealed significant hydroxyapatite layer growth on TiO_2-coated NiTi, especially at a sputtering power of 240 W. Reduced nickel ion release was observed on TiO_2 nanoparticles with a thickness of 21.90 nm at 50 W sputtering power compared with 31.93 nm-thick nanoparticles at 240 W. Ta_2O_5 thin films were deposited on NiTi substrates through DC magnetron reactive sputtering at ~100 °C with a deposition power of 50 W. Structural and morphological analyses through optical microscopy and X-ray diffraction, atomic force microscopy, and scanning electron microscopy revealed the homogeneity and low roughness of the coatings. Biocompatibility assessments in artificial saliva and SBF solutions established that Ta_2O_5-coated NiTi alloys exhibited superior electrochemical behavior, enhanced corrosion resistance, and diminished Ni ion release compared with uncoated specimens. Conclusion: TiO_2 and Ta_2O_5 coatings not only improved the biocompatibility of NiTi orthodontic archwires but also presented a promising path for advanced biomedical applications. These coatings have potential in improving the cellular behavior and performance of NiTi-based orthodontic devices.

Keywords: *Nickel-titanium, Orthodontic archwires, Nanoparticle, TiO_2, Ta_2O_5, atomic force microscopy, scanning electron microscopy, artificial saliva.*

Introduction

Biomaterials derived from natural or synthetic sources play a pivotal role in modern medical practices. These materials are meticulously engineered to interact seamlessly with biological systems, including tissues, blood, and biological fluids, without inducing adverse effects on the host. Applications of biomaterials span a wide range of medical fields, from prosthetic devices and diagnostics to treatments and storage [1–4]. In dentistry and orthodontics, biomaterials are integral to enhancing and maintaining oral health and aesthetic outcomes. The core principle of orthodontic treatments rests on a mechanical foundation, positing that intentional manipulation of tooth movement can effectively convert stored elastic energy into mechanical work. For precise control, orthodontic wires are indispensable components [5]. Fixed orthodontic treatments have a rich history of utilizing orthodontic wires, which are designed to conform to dental arches and rectify tooth misalignments. Various wires made of alloys are available, each offering distinct attributes aimed at shortening treatment duration and elevating patient comfort [6,7].

Orthodontic wires should possess certain key attributes to be optimally effective. Given their persistent, intimate contact with the oral environment, these materials should exhibit corrosion resistance, minimize ion release into the oral cavity, and be non-allergenic. Establishing harmonious interactions between dental tissues and orthodontic wires is paramount [8]. Nickel–titanium (NiTi) alloy has gained significant attention in biomedical applications, especially in orthodontics. This alloy is known for its unique properties, such as shape memory effect, superelasticity, and superior biocompatibility [9]. Its versatility has led to its use across multiple medical specialties, including cardiology and neurosurgery [10–14]. The term "biocompatibility" stands central in the context of biomaterials and refers to a material's capability to fulfil its intended application without eliciting undesirable host responses [10]. Achieving biocompatibility is vital for the successful integration of biomaterials in therapeutic scenarios.

In orthodontics, NiTi wires, especially those in the austenitic phase at oral temperatures (37 °C), are effective when paired with orthodontic brackets. The adoption of NiTi wires in orthodontic procedures is attributed to their superelastic characteristics, which facilitate consistent and gentle force applications, thereby ensuring effective tooth movements [10]. NiTi alloys are also applied to vascular stents due to their notable anti-thrombotic features and unmatched biocompatibility [15,16]. The success of these self-expandable stents in treating atherosclerotic lesions across various arterial pathways underscores their efficacy. However, concerns arise with the prolonged use of NiTi orthodontic wires under tensile stress, especially concerning potential nickel ion release, emphasizing the importance of biocompatibility [17]. To address these challenges, researchers have explored various strategies, including the formation of inert oxide layers on NiTi surface through post-surface treatment techniques. These methods can enhance the biocompatibility and surface resilience and greatly contribute to the overall effectiveness of these biomaterials [18–22]. This study aims to elevate the biocompatibility of NiTi alloy by developing a new coating using TiO_2 and Ta_2O_5 through direct current (DC) reactive sputtering technology.

Materials and Methods

Preparation of samples

Circular NiTi alloy sheets measuring 15 mm in diameter and 2 mm in thickness were prepared by cutting. The specimens were cleaned thoroughly with running water to ensure their cleanliness and remove any impurities caused by environmental factors. The surface of the specimens was meticulously prepared by grinding with silicon carbide paper, followed by polishing using a specialized cloth. The specimens were immersed in high-purity alcohol with a purity level of 99% and subjected to 30 minutes of ultrasonic vibration for optimal surface treatment at 100 °C.

Coating procedure

Sputtering was conducted using a DC magnetron reactive sputtering system (CRC-600 system, Torr Inc., USA) employing a high-purity titanium target with a diameter of 5 mm and a thickness of 3 mm that was affixed to a balanced magnetron. A DC sputtering plasma machine was operated to generate TiO_2 layers with varying thicknesses by applying different sputtering power levels of 50–240 W, and the deposition duration was set at 120 minutes. The initial chamber pressure was set at 1×10^{-5} mbar and subsequently increased to 1×10^{-2} mbar by introducing high-purity argon gas into the chamber. Prior to coating, the titanium target underwent an initial exposure to continuous plasma to ensure a clean surface to form a TiO_2 and Ta_2O_5 nanostructure on the NiTi substrate.

Characterization

X-ray diffraction (XRD) measurements were conducted using a Shimadzu X-ray diffractometer with a wavelength of 1.54056 Å to detect phases present in the specimens. The surface morphology of the samples was assessed through field emission scanning electron microscopy (FESEM, Hitachi S-4160 scanning electron microscope) under the magnification range of 10,000x to 50,000x. An energy-dispersive X-ray spectrometer (EDXS) unit integrated with the FESEM was operated to determine the elemental composition of the TiO_2 coating layer. The release of nickel ions was quantified by measuring the nickel

ion content in artificial saliva (AS) solutions. All the specimens were immersed statically in separate containers filled with 100 ml of AS solutions for 14 days. Nickel ion concentration was determined using graphite-furnace atomic absorption spectrometry (GFAAS) (AA6501F, Shimadzu, Japan).

Results

Microstructural characterization

The NiTi alloy specimens underwent reinforcement with an initial TiO_2 and Ta_2O_5 layer to enhance their biocompatibility. Various DC sputtering powers (50, 180, 200, and 240 W) were applied to deposit the TiO_2 and Ta_2O_5 coating layer. The thickness of the TiO_2 thin films was precisely determined using an optical interferometer method. The thicknesses of the TiO_2 and Ta_2O_5 thin films were 105.3, 108, 135.2, and 120.4 nm.

Figures (1 to 5) illustrate the FESEM images of the TiO2 and Ta2O5 thin coating layers deposited on the NiTi specimens at various sputtering powers. Specifically, Figures 1 and 2 show the NiTi specimens sputtered with TiO2 at 50 W and 100 W, respectively, while Figures 3 and 4 display the NiTi specimens sputtered with Ta2O5 at 150 W and 180 W, respectively. Figure 5 demonstrates the uniform, homogeneous distribution of Ta2O5 nanoparticles on the NiTi specimen sputtered at the optimal 200 W. This particular specimen, compared to those sputtered at lower powers, exhibits the highest quality film with a more uniform and homogeneous coating, indicating that a sputtering power of 200 W is most effective for Ta2O5 deposition, though it results in the lowest growth rate compared to TiO2 and TiN coatings on other specimens.

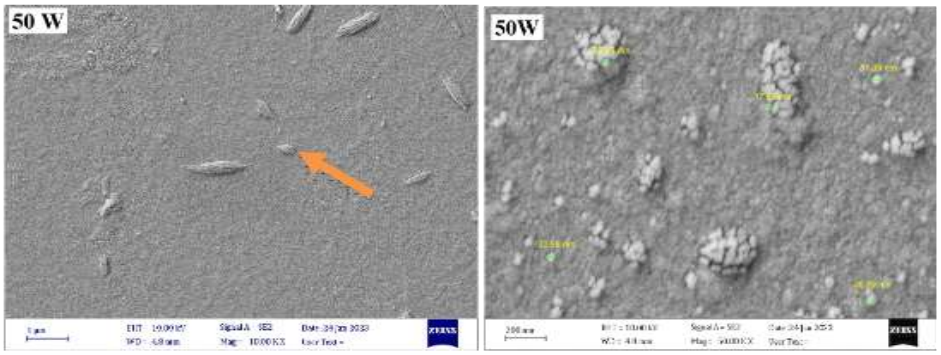

Figure 1: FESEM image for TiO_2 nanoparticles coating layer deposited with sputtering power of 50 W

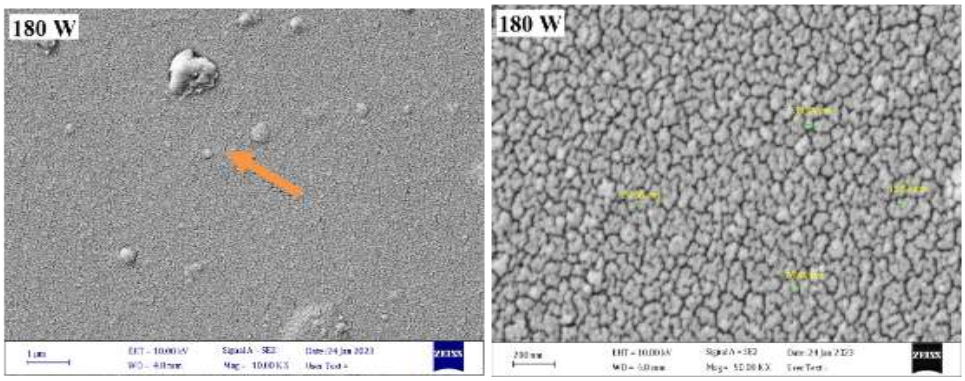

Figure 2: FESEM image for TiO_2 nanoparticles coating layer deposited with sputtering power of 180 W

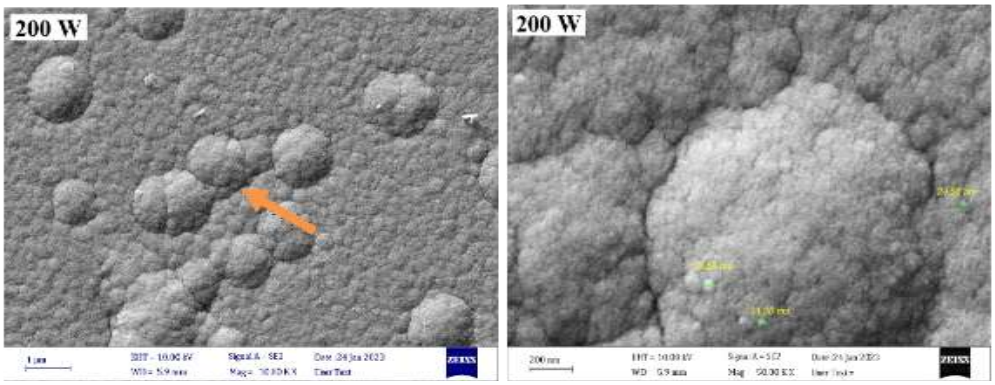

Figure 3: FESEM image for TiO_2 nanoparticles coating layer deposited with sputtering power of 200 W

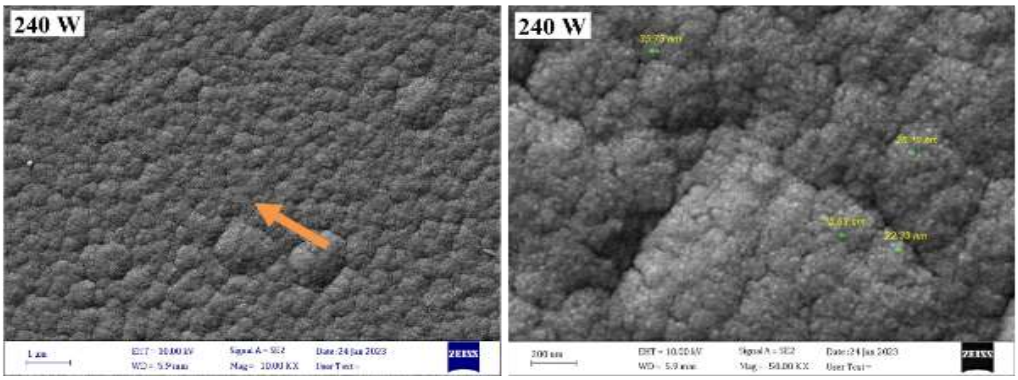

Figure 4: FESEM image for TiO_2 nanoparticles coating layer deposited with sputtering power of 240 W

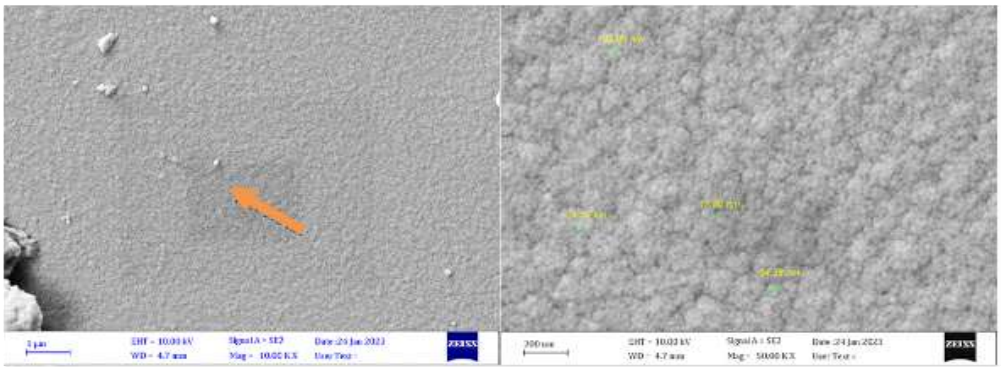

Figure 5: FESEM image for Ta_2O_5 nanoparticles coating layer deposited with sputtering power of 200 W

Biocompatibility measurements

Optical microscopy and XRD analyses were conducted on the uncoated NiTi alloy substrate and the TiO_2/NiTi and Ta_2O_5/NiTi structure to assess their potential biocompatibility. The first biocompatibility assessment involved immersing the specimens in simulated body fluid (SBF), similar to AS, for 1 month. The optical microscope images of the coated TiO_2/NiTi and Ta_2O_5 /NiTi structure and the uncoated NiTi alloy substrate after this immersion period are presented in Figures (6a-e) and Figure (6f), respectively. Figures 7 and 8 show the XRD patterns for all specimens, namely, uncoated NiTi and coated with TiO_2 and Ta_2O_5 layers, immersed in AS for 1 month.

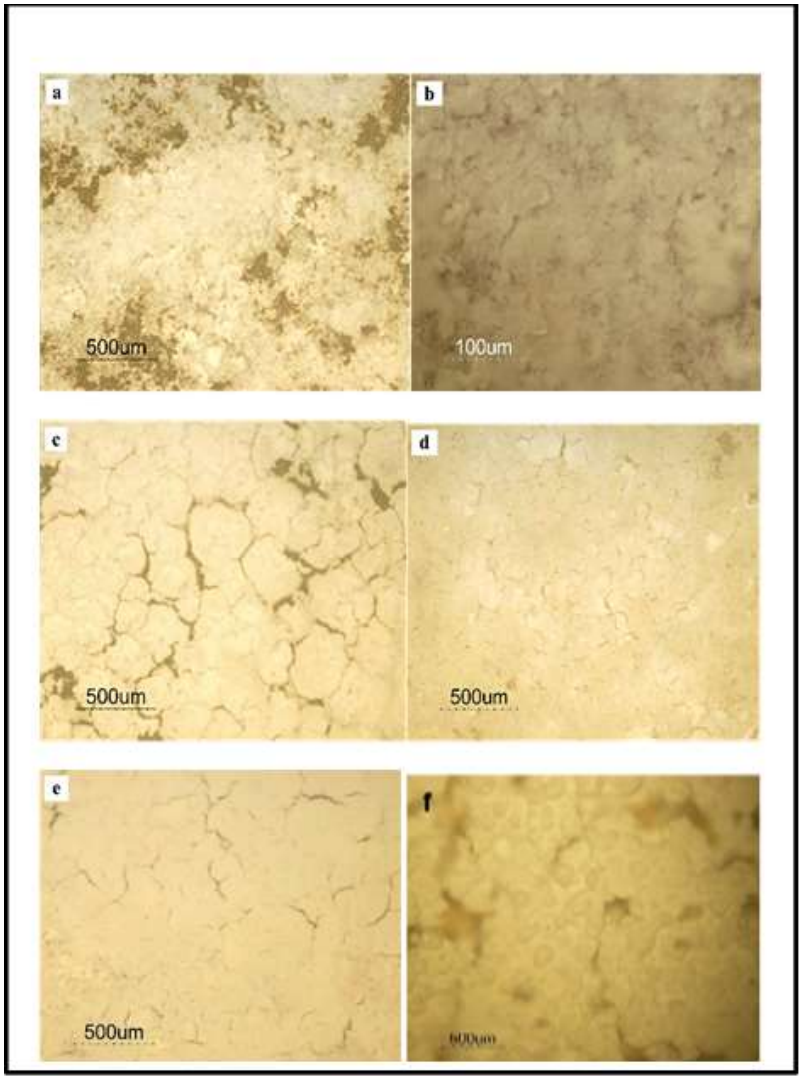

Figure 6: Optical microscopy images for all specimens after biocompatibility test: a: base (uncoated NiTi), NiTi coated with b: TiO_2 (50 W), c: TiO_2 (180 W), d: TiO_2 (200 W), e: TiO_2 (240 W), and f: Ta_2O_5 (200 W)

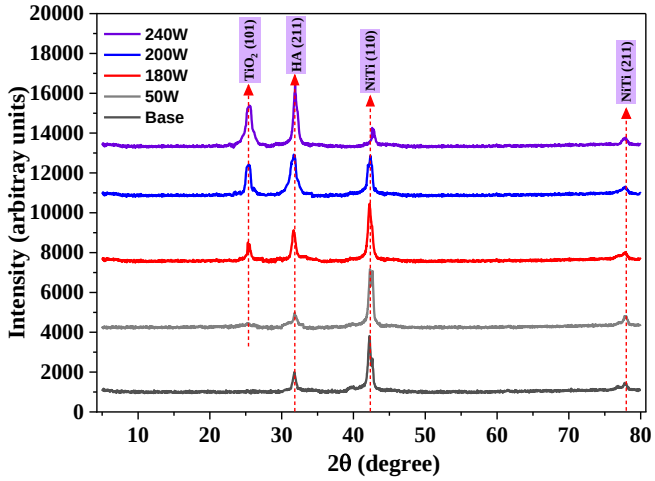

Figure 7: XRD patterns after the biocompatibility testing of NiTi Alloys. Comparison of uncoated and TiO_2-coated specimens at varied sputtering powers (50, 180, 200, and 240 W)

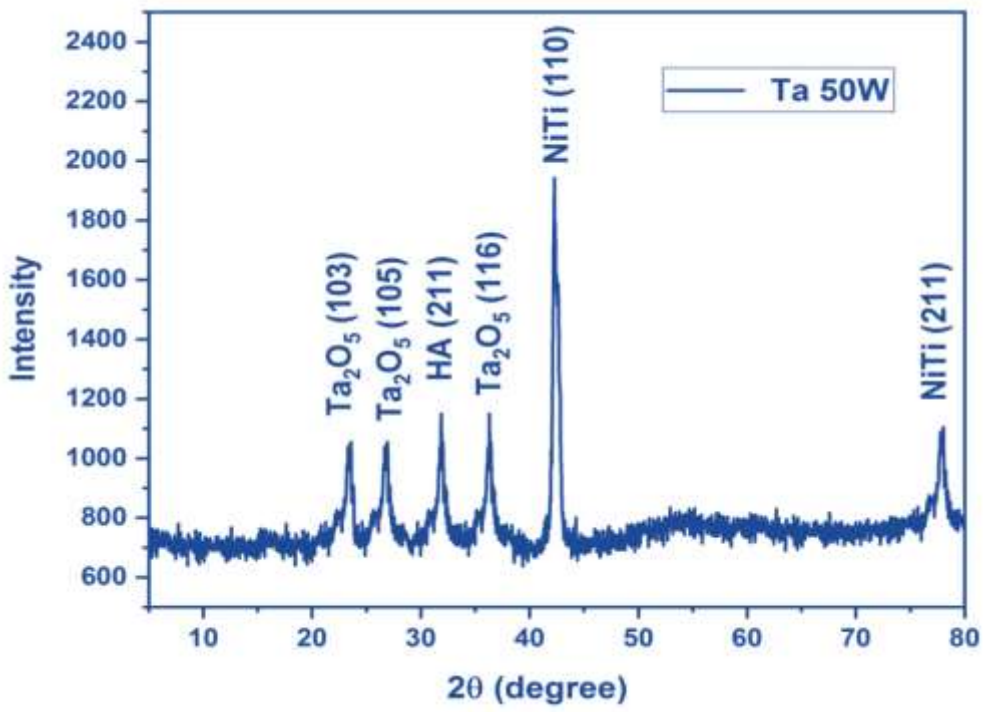

Figure 8: XRD patterns after the biocompatibility assessment of NiTi alloy specimens coated with Ta_2O_5 layer

Release of Ni ion

Experiment was conducted to address Ni ion release by using sputter-coated TiO_2 and Ta_2O_5 films onto NiTi substrate. Nickel ions leached from the substrates during the electrochemical tests were determined to assess the effectiveness of the sputter-coated surface to impede out-diffusion. The solutions taken from each specimen after the corrosion test were analyzed for Ni concentrations using atomic absorption spectroscopy (AAS). Static immersion experiments were carried out on sputter-coated TiO_2 and Ta_2O_5 films on NiTi substrates in AS solutions. The Ni ions were released during corrosion in the physiological environment.

Table 1 illustrates the variations in the amount of Ni ions released for uncoated and coated NiTi specimens immersed in AS solution. All specimens were statically immersed in 100 ml of AS solutions in separate containers for 14 days. The chemical compositions of AS solutions are provided in the previous experimental part. Immersion experiments were performed at 37 ± 0.5 °C in an electronically controlled water bath to simulate the body temperature. As shown in Table 1, following an immersion period of 14 days in AS, the Ni ion released from the TiO_2-coated NiTi was about half of that from the uncoated NiTi. The Ni ion released from the Ta_2O_5-coated specimens was lower than that from the uncoated samples.

Table 1: Concentration of released Ni ions in the AS solutions of TiO_2 and Ta_2O_5 coatings layer deposited onto NiTi substrates at different sputtering powers

Coating materials	Sputtering Power (W)	Coating layer thickness (nm)	Ni concentrations (ppb)
Base (un-coated NiTi)			66.6
TiO_2/NiTi	50	100	38.8
TiO_2/NiTi	180	112	44.4
TiO_2/NiTi	200	135	50
TiO_2/NiTi	240	120	61.6
Ta_2O_5/NiTi	200	119	55.5

Discussion

Optical interferometry was used to determine the thickness of TiO_2 thin films. At sputtering power levels of 50, 180, 200, and 240 W, the thicknesses of the TiO_2 thin films were observed to be 105.3, 108, 135.2, and 120.4 nm, respectively. An increase in thin film thickness with escalating sputtering power can be linked to the surge in the concentration of charged particles. Increasing the DC sputtering power provides more reactants with increased energy, potentially resulting in a denser layer. Lower sputtering powers tend to have a diminished deposition rate due to the less energized argon interacting with target species and the subsequent reduction in the number of atoms ejected from the target material. However, as the sputtering power increases, the yield of the TiO_2 film coating significantly increases. The film's growth rate accelerates with the increase in sputtering power, peaking at 200 W, but this growth does not follow a straightforward route. A decrease in the film growth rate at a sputtering power of 240 W might be attributed to re-sputtering due to high-energy sputtered flux [23].

For XRD measurements, the TiO_2 coating layer deposited at higher sputtering power exhibited an intensified (101) peak in comparison with those generated at lower sputtering power [24]. The magnitude of this peak in the X-ray diffraction pattern serves as a direct metric for film crystallinity. The augmented peak intensity at elevated sputtering power could be due to the increased surface mobility of adatoms with more substantial energy, coupled with the increase in argon sputtering power [25]. This combination is crucial to obtain a highly crystalline coating layer. A higher power ensures that atoms have more available energy to facilitate diffusion and optimal settling within the crystal lattice. Chan and Teo [26] provided evidence that larger crystallite sizes, up to 1 μm, can be accurately measured using the Scherrer equation under certain conditions, such as using diffraction peaks at higher 2θ angles. However, as the sputtering power increased to the range of 200–240W, the peak not only intensified but also broadened. This finding might suggest alterations in the phase or crystalline structure due to changing deposition parameters. Crystallinity was determined using the full width at half maximum (FWHM) intensity of the (101) peak by applying the Scherrer equation [27]. A narrower FWHM suggests better crystallinity, as indicated by Panjan et al [28]. Among the specimens, the TiO_2 film deposited at a sputtering power of 240 W exhibited the most distinct (101) peak intensity and the narrowest FWHM compared with the films coated within 50–200 W [29]. The data suggest a direct correlation between the crystallinity of the film coatings and the operational sputtering power [30]. This relationship could be linked to the increased density of surface atoms, which, under elevated power, are swiftly released and spread across the substrate. However, at excessively high sputtering power, the rapid growth rate might lead to the dispersion of previously deposited particles across the substrate's surface [31]. The subsequent particles overlaying these could compromise the crystalline structure of the TiO_2 film coating [32].

The TiO_2 film coatings produced within the sputtering power range of 50–240 W showed the most distinct peak intensity and the narrowest FWHM compared with other TiO_2 films [33]. The TiO_2 film deposited at 240 W possessed superior crystalline quality. This observation can be traced back to the sputtering yields associated with TiO_2 and Ta_2O_5 [34].

This study also evaluated the particle size corresponding to each sputtering power. The particle size was maximal at a sputtering power of 200 W, declining as the sputtering power elevated [35]. Typically, the particle size of thin film coatings is directly correlated with crystallinity [36]. Given the reduction in particle size with the rise in sputtering power, it was expected that the crystallinity of the films would decrease as the sputtering power augmented [37]. To corroborate this hypothesis, the crystallinity of the TiO_2 film coating was examined using XRD.

After a month of immersion in synthetic simulated body fluid (SBF) for biocompatibility tests, optical microscope images of the uncoated and coated NiTi specimens immersed in SBF were analyzed [38]. A hydroxyapatite layer grew on the surfaces of all specimens, indicative of biocompatibility from the simulated body fluid, thereby affirming the biocompatibility of the coating layer [39]. The optical microscope test displayed the presence of agglomerated hydroxyapatite after immersion [40]. From the

microscopy images, significant agglomeration of hydroxyapatite in specimens coated with Ta_2O_5 (200 W) and TiO_2(240 W) was evident, aligning with XRD findings [41]. Lesser agglomeration was observed in specimens coated with TiO_2 (200 W) and TiO_2 (180 W), while the least agglomeration was seen in specimens coated with TiO_2 (50 W) and uncoated base material [42]. The XRD test indicated the presence of a hydroxyapatite peak in all patterns [43]. As shown, the representative XRD pattern for the NiTi alloy uncoated base specimen exhibited a hydroxyapatite peak at $2\theta = 31.78$, corresponding to the standard XRD pdf card ICDD 09-0432 for hydroxyapatite [44]. This peak, derived from the biomimetic formation of hydroxyapatite from SBF, signifies biocompatibility and osseointegration [45]. The TiO_2 peaks appeared at 2θ = 25.28, 25.29, 25.23, and 25.24, coinciding with the standard XRD pdf card ICDD 21-1272 for anatase titanium oxide [46]. The comparison of the XRD patterns for all coated NiTi specimens with the uncoated one showed a noticeable increase in hydroxyapatite peak intensity and TiO_2 anatase peak [47].

Conclusion

In this study, magnetron sputtering was used to apply TiO_2 and Ta_2O_5 coatings onto nickel-titanium surfaces for potential use in orthodontic archwires. These coatings improved the biological safety and physical properties of NiTi. The biocompatibility was confirmed through biomimetic synthesis from synthetic simulated body fluid (SBF). The TiO_2 coating remarkably enhanced hydroxyapatite formation, while the Ta_2O_5-coated specimens demonstrated strong corrosion resistance in acidic saliva. Collectively, these coatings on NiTi offer promising advancements for orthodontic materials, combining durability, biocompatibility, and reduced cytotoxic risks.

Conflict of interest:

The authors have no conflicts of interest to declare.

Author Contributions

Conceptualization, Data curation, investigation, methodology, validation, and writing – original draft, were all carried out by Abeer Basim Mahmood. Visualization, review & editing were carried out by Akram Faisal Alhuwaizi, Mohammed K. Khalaf, Abbas R. Zaher.

Acknowledgements

The authors thank researchers in the Centre of Applied Physics of the Directorate of Materials Research, Ministry of Science and Technology, Baghdad, Iraq, for their continuous help and support.

References

1. AlQuraini N, Shah R, Cunningham SJ. Perceptions of outcomes of orthodontic treatment in adolescent patients: a qualitative study. Eur J Orthod. 2019;41(3):294–300. http://dx.doi.org/10.1093/ejo/cjy071

2. Katada H. Esthetic Improvement through Orthodontic Treatment Involving Extraction: Use of Orthodontic Anchor Screws. Bull Tokyo Dent Coll. 2018;60(2):115–29. http://dx.doi.org/10.2209/tdcpublication.2018-0041

3. Al-Khatieeb MM, Mohammed SA, Al-Attar AM. Evaluation of a New Orthodontic Bonding System: Beauty Ortho Bond. J Bagh Coll Dent. 2015;27(1):175–81. http://dx.doi.org/10.12816/0015284

4. Abid M, Alhuwaizi A, Al-Attar A. Do orthodontists aim to decrease the duration of fixed appliance treatment? J Orthod Sci. 2021;10(1):6. http://dx.doi.org/10.4103/jos.jos_36_20

5. Saloom HF, Papageorgiou SN, Carpenter GH, Cobourne MT. Impact of Obesity on Orthodontic Tooth Movement in Adolescents: A Prospective Clinical Cohort Study. J Dent Res. 2017;96(5):547–54. http://dx.doi.org/10.1177/0022034516688448

6. Kareem YM, Hamad TI, AL-Rawas M. Evaluating the effect of barium titanate nanofiller addition on the thermal conductivity and physio-mechanical properties of maxillofacial silicone. J Bagh Coll Dent. 2024;36(2):20–33. http://dx.doi.org/10.26477/jbcd.v36i2.3674

7. Alkhawaja HAA, Al Haidar AHMJ. Effect of a novel coating material on the microleakage of glass hybrid restoration in primary teeth – An in vitro study. J Bagh Coll Dent. 2023;35(1):20–6. http://dx.doi.org/10.26477/jbcd.v35i1.3311

8. Castro SM, Ponces MJ, Lopes JD, Vasconcelos M, Pollmann MCF. Orthodontic wires and its corrosion—The specific case of stainless steel and beta-titanium. J Dent Sci. 2015;10(1):1–7. http://dx.doi.org/10.1016/j.jds.2014.07.002

9. Sifakakis I, Eliades T. Adverse reactions to orthodontic materials. Aust Dent J. 2017;62(S1):20–8. http://dx.doi.org/10.1111/adj.12473

10. Ratner BD. A pore way to heal and regenerate: 21st century thinking on biocompatibility. Regen Biomater. 2016;3(2):107–10. http://dx.doi.org/10.1093/rb/rbw006

11. Pilar Shetty B, Subramanya R, Reddy S, Shetty V. An overview on biocompatibility and failure analysis of acrylonitrile butadiene steryene based laryngoscope. Suranaree J Sci Technol. 2023;30(1):010192(1-9). http://dx.doi.org/10.55766/sujst-2023-01-e01876

12. Li Q, Zeng Y, Tang X. The applications and research progresses of nickel–titanium shape memory alloy in reconstructive surgery. Australas Phys Eng Sci Med. 2010;33(2):129–36. http://dx.doi.org/10.1007/s13246-010-0022-8

13. Sharma N, Jangra K, Raj T. Applications of Nickel-Titanium Alloy. J Eng Technol. 2015;5(1):1. http://dx.doi.org/10.4103/0976-8580.149472

14. Singh A, Sharma S, Batra P, Arora N, Kannan S. Effects of different storage temperatures on the properties of nonlatex orthodontic modules. Indian J Dent Res. 2022;33(4):350. http://dx.doi.org/10.4103/ijdr.ijdr_453_22

15. Tan L, Crone WC. Surface characterization of NiTi modified by plasma source ion implantation. Acta Mater. 2002;50(18):4449–60. http://dx.doi.org/10.1016/s1359-6454(02)00251-3

16. Nazarahari A, Canadinc D. Prediction of the NiTi shape memory alloy composition with the best corrosion resistance for dental applications utilizing artificial intelligence. Mater Chem Phys. 2021;258:123974. http://dx.doi.org/10.1016/j.matchemphys.2020.123974

17. Quazi MM, Ishak M, Fazal MA, Arslan A, Rubaiee S, Aiman MH, et al. A comprehensive assessment of laser welding of biomedical devices and implant materials: recent research, development and applications. Crit Rev Solid State Mater Sci. 2020;46(2):109–51. http://dx.doi.org/10.1080/10408436.2019.1708701

18. Nsaif YA, Mahmood AB. Effect of Fluoride Agent on the Load Deflection of Rhodium-Coated Arch Wires; An In-Vitro Study. Indian J Public Health Res Dev. 2019;10(2):823. http://dx.doi.org/10.5958/0976-5506.2019.00397.8

19. Mahmood AB. Coated stainless steel archwires' discoloration measured by computerized system (An in-vitro study). J Bagh Coll Dent. 2020;32(4):1–4. http://dx.doi.org/10.26477/jbcd.v32i4.2911

20. Mohsin SK. An Evaluation of Corrosion Pits in Esthetic Coated Stainless Steel Orthodontic Archwires in Dry and Wet Environment at Different Intervals: An in Vitro Study. J Bagh Coll Dent. 2016;28(1):153–7. http://dx.doi.org/10.12816/0024726

21. Muayad NS, Ghaib NH. The Effect of Artificial Saliva on the Surface Roughness of Different Esthetic Archwires: An in Vitro Study. J Bagh Coll Dent. 2017;29(3):106–12. http://dx.doi.org/10.12816/0041190

22. Gao W, Li Z. ZnO thin films produced by magnetron sputtering. Ceram Int. 2004;30(7):1155–9. http://dx.doi.org/10.1016/j.ceramint.2003.12.197

23. Xu Y, Li G, Li G, Gao F, Xia Y. Effect of bias voltage on the growth of super-hard (AlCrTiVZr)N high-entropy alloy nitride films synthesized by high power impulse magnetron sputtering. Appl Surf Sci. 2021;564:150417. http://dx.doi.org/10.1016/j.apsusc.2021.150417

24. Chan KY, Teo BS. Effect of Ar pressure on grain size of magnetron sputter-deposited Cu thin films. IET Sci Meas Technol. 2007;1(2):87–90. http://dx.doi.org/10.1049/iet-smt:20060110

25. Zhou Y, Zheng HF, Zhao G, Li M, Liu BT. Influence of Sputtering Power on Structural and Optical Properties of ZnO Films Fabricated by RF Magnetron Sputtering. Adv Mater Res. 2014;1053:325–31. http://dx.doi.org/10.4028/www.scientific.net/amr.1053.325

26. Muniz FTL, Miranda MAR, Morilla dos Santos C, Sasaki JM. The Scherrer equation and the dynamical theory of X-ray diffraction. Acta Crystallogr A Found Adv. 2016;72(3):385–90. http://dx.doi.org/10.1107/s205327331600365x

27. Cougnon F, Depla D. The Seebeck Coefficient of Sputter Deposited Metallic Thin Films: The Role of Process Conditions. Coatings. 2019;9(5):299. http://dx.doi.org/10.3390/coatings9050299

28. Panjan P, Drnovšek A, Gselman P, Čekada M, Panjan M. Review of Growth Defects in Thin Films Prepared by PVD Techniques. Coatings. 2020;10(5):447. http://dx.doi.org/10.3390/coatings10050447

29. Ulkareem MA, Noori FTM, Khalaf MK. Corrosion resistance of Ti6Al4V alloy by Radio Frequency Technique used for Coating Deposition of multilayer (HA/TiN/Ti6Al4V-substrate) for Optimization power. IOP Conf Ser Mater Sci Eng. 2020;757(1):012047. http://dx.doi.org/10.1088/1757-899x/757/1/012047

30. Amor SB, Baud G, Besse JP, Jacquet M. Structural and optical properties of sputtered Titania films. Mater Sci Eng B. 1997;47(2):110–8. http://dx.doi.org/10.1016/s0921-5107(97)00027-5

31. Ohya S, Chiaro B, Megrant A, Neill C, Barends R, Chen Y, et al. Room temperature deposition of sputtered TiN films for superconducting coplanar waveguide resonators. Supercond Sci Technol. 2013;27(1):015009. http://dx.doi.org/10.1088/0953-2048/27/1/015009

32. Hrbek J. Sputtering of metals in the presence of reactive gases. Thin Solid Films. 1977;42(2):185–191. http://dx.doi.org/10.1016/0040-6090(77)90416-3

33. Soltabayev B, Yergaliuly G, Ajjaq A, Beldeubayev A, Acar S, Bakenov Z, et al. Quick NO Gas Sensing by Ti-Doped Flower–Rod-like ZnO Structures Synthesized by the SILAR Method. ACS Appl Mater Interfaces. 2022;14(36):41555–70. http://dx.doi.org/10.1021/acsami.2c10055

34. Torres-Costa V, Martín-Palma RJ. Optical properties of porous silicon materials. Porous Silicon Biomed Appl. 2021;183–222. http://dx.doi.org/10.1016/b978-0-12-821677-4.00008-2

35. Kumar Rajak D, Pagar DD, Menezes PL, Eyvazian A. Friction-based welding processes: friction welding and friction stir welding. J Adhes Sci Technol. 2020;34(24):2613–37. http://dx.doi.org/10.1080/01694243.2020.1780716

36. Bae D, Gho J, Shin M, Kwon S. Effect of zinc addition on properties of cadmium sulfide layer and performance of Cu(In,Ga)Se2 solar cell. Thin Solid Films. 2013;535:162–165. http://dx.doi.org/10.1016/j.tsf.2012.11.077

37. Welzel U, Ligot J, Lamparter P, Vermeulen AC, Mittemeijer EJ. Stress analysis of polycrystalline thin films and surface regions by X-ray diffraction. J Appl Crystallogr. 2005;38(1):1–29. http://dx.doi.org/10.1107/s0021889804029516

38. Rauuf AF, Aadim KA. Effect of Annealing Times on the Structural and Optical Properties of PbO Thin Films Prepared by D.C Sputtering. Iraqi J Sci. 2023;2877–88. http://dx.doi.org/10.24996/ijs.2023.64.6.18

39. Lee JH, Jang HL, Lee KM, Baek HR, Jin K, Hong KS, et al. In vitro and in vivo evaluation of the bioactivity of hydroxyapatite-coated polyetheretherketone biocomposites created by cold spray technology. Acta Biomater. 2013;9(4):6177–87. http://dx.doi.org/10.1016/j.actbio.2012.11.030

40. Al-Hasan R, Al-Taee L. Interfacial Bond Strength and Morphology of Sound and Caries-affected Dentin Surfaces Bonded to Two Resin-modified Glass Ionomer Cements. Oper Dent. 2022;47(4):E188–E196.. http://dx.doi.org/10.2341/21-048-l

41. Al-Oubidy EA, Kadhim FJ. Photocatalytic activity of anatase titanium dioxide nanostructures prepared by reactive magnetron sputtering technique. Opt Quantum Electron. 2019;51(1). http://dx.doi.org/10.1007/s11082-018-1738-z

42. Firouzabadi SS, Naderi M, Dehghani K, Mahboubi F. Effect of nitrogen flow ratio on nano-mechanical properties of tantalum nitride thin film. J Alloys Compd. 2017;719:63–70. http://dx.doi.org/10.1016/j.jallcom.2017.05.159

43. Durante O, Di Giorgio C, Granata V, Neilson J, Fittipaldi R, Vecchione A, et al. Emergence and Evolution of Crystallization in TiO2 Thin Films: A Structural and Morphological Study. Nanomaterials. 2021;11(6):1409. http://dx.doi.org/10.3390/nano11061409

44. Taratuta A, Lisoń-Kubica J, Paszenda Z, Szewczenko J, Kazek-Kęsik A, Opilski Z, et al. Influence of passive layer fabrication method on physicochemical and antimicrobial properties of the Ta2O5 layer on NiTi alloy. Vacuum. 2023;214:112187. http://dx.doi.org/10.1016/j.vacuum.2023.112187

45. Guillén C, Herrero J. TiO2 coatings obtained by reactive sputtering at room temperature: Physical properties as a function of the sputtering pressure and film thickness. Thin Solid Films. 2017;636:193–199. http://dx.doi.org/10.1016/j.tsf.2017.05.048

46. Ramos-Corella KJ, Sotelo-Lerma M, Gil-Salido AA, Rubio-Pino JL, Auciello O, Quevedo-López MA. Controlling crystalline phase of TiO2 thin films to evaluate its biocompatibility. Mater Technol. 2019;34(8):455–62. http://dx.doi.org/10.1080/10667857.2019.1576821

47. Gupta BK, Kulshrestha S, Agarwal AK. Friction and wear behavior of ion-plated lead–tin coatings. J Vac Sci Technol A. 1987;5(3):358–63. http://dx.doi.org/10.1116/1.574160

تقييم جسيمات التيتانيوم النانوية وجسيمات التانتالوم النانوية على تغليف أسلاك النيكل تيتانيوم في تقويم الأسنان (دراسة في المختبر)

عبير باسم محمود ,أكرم فيصل الحويزي , محمد خماس خلف , عباس رفيق زاهر

المستخلص:

الخلفية: هذه الدراسة تتناول تحسين خصائص سطح أسلاك تقويم الأسنان من النيكل-التيتانيوم (NiTi) باستخدام مادتي تغليف متميزتين: ثاني أكسيد التيتانيوم (TiO_2) وبنتاوم بنتاوكساید (Ta_2O_5). بالنسبة للأولى، تم ترسيب جسيمات TiO_2 النانوية بسماكات تتراوح بين 21.90 نانومتر إلى 31.93 نانومتر على أسطح سبائك NiTi باستخدام تقنية الرش الاستجابي بالتيار المستمر (DC) بشروط طاقة متغيرة. تحقق تشتت الأشعة السينية والمجهر الإلكتروني ذو الإشعة الميدانية (FESEM) من توحيدية وشكل التغليف. أظهرت اختبارات الانغمار في سائل الجسم المشبع بالمحاليل الاصطناعية (SBF) نمو طبقة هيدروكسيابات ملحوظة على الأسلاك المغطاة بـ TiO_2، خاصةً عند طاقة رش قدرها 240 واط. يجدر بالذكر أنه تم ملاحظة انخفاض إطلاق أيونات النيكل مع جسيمات TiO_2 بسمك 21.90 نانومتر عند طاقة رش 50 واط مقارنة بتلك بسمك 31.93 نانومتر عند طاقة رش 240 واط. أما بالنسبة للثانية، تم ترسيب أفلام رقيقة من Ta_2O_5 على أسطح NiTi باستخدام تقنية الرش المغناطيسي المستجيب بالتيار المستمر (DC) عند درجة حرارة تقريبية تبلغ 100 درجة مئوية مع طاقة ترسيب قدرها 50 واط. أظهرت التحليلات الهيكلية والمورفولوجية، بما في ذلك تشتت الأشعة السينية، ومجهر القوة الذرية (AFM)، ومجهر المسح الإلكتروني (SEM) توحيدية ونعومة التغليف. أثبتت تقييمات التوافق مع اللعاب الاصطناعي المخلوط (AS) وسائل الجسم المشبعة (SBF) أن السبائك المغطاة بـ Ta_2O_5 أظهرت سلوكًا كهروكيميائيًا متفوقًا، ومقاومة تآكل معززة، وإطلاق أقل لأيونات النيكل، مقارنة بالعينات غير المغطاة. في الختام، تظهر تغليفات TiO_2 وTa_2O_5 على أسلاك تقويم الأسنان NiTi ليس فقط تعزيز توافقها مع الجسم ولكن أيضًا تقديم طريقة واعدة لتطبيقات التكنولوجيا الحيوية المتقدمة، مؤكدة على إمكانية هذه التغليفات في تحسين سلوك الخلايا وأداء أجهزة تقويم الأسنان القائمة على NiTi.